N73-21453

NASA TECHNICAL NOTE

NASA TN D-7173

NASA TN D-7173

CASE FILE COPY

EFFECT OF SPECIMEN THICKNESS ON FATIGUE-CRACK-GROWTH BEHAVIOR AND FRACTURE TOUGHNESS OF 7075-T6 AND 7178-T6 ALUMINUM ALLOYS

by C. Michael Hudson and J. C. Newman, Jr.

Langley Research Center
Hampton, Va. 23365

NATIONAL AERONAUTICS AND SPACE ADMINISTRATION • WASHINGTON, D. C. • APRIL 1973

1. Report No.	2. Government Accession No.	3. Recipient's Catalog No.
NASA TN D-7173		

4. Title and Subtitle
EFFECT OF SPECIMEN THICKNESS ON FATIGUE-CRACK-GROWTH BEHAVIOR AND FRACTURE TOUGHNESS OF 7075-T6 AND 7178-T6 ALUMINUM ALLOYS

5. Report Date
April 1973

6. Performing Organization Code

7. Author(s)
C. Michael Hudson and J. C. Newman, Jr.

8. Performing Organization Report No.
L-8731

10. Work Unit No.
501-22-02-01

9. Performing Organization Name and Address
NASA Langley Research Center
Hampton, Va. 23365

11. Contract or Grant No.

13. Type of Report and Period Covered
Technical Note

12. Sponsoring Agency Name and Address
National Aeronautics and Space Administration
Washington, D.C. 20546

14. Sponsoring Agency Code

15. Supplementary Notes

16. Abstract

A study was made to determine the effects of specimen thickness on fatigue-crack growth and fracture behavior of 7075-T6 and 7178-T6 aluminum-alloy sheet and plate. Specimen thicknesses ranged from 5.1 to 12.7 mm (0.20 to 0.50 in.) for 7075-T6 and from 1.3 to 6.4 mm (0.05 to 0.25 in.) for 7178-T6. The stress ratios R used in the crack-growth experiments were 0.02 and 0.50. For 7075-T6, specimen thickness had relatively little effect on fatigue-crack growth. However, the fracture toughness of the thickest gage of 7075-T6 was about two-thirds of the fracture toughness of the thinner gages of 7075-T6. For 7178-T6, fatigue cracks generally grew somewhat faster in the thicker gages than in the thinnest gage. The fracture toughness of the thickest gage of 7178-T6 was about two-thirds of the fracture toughness of the thinner gages of 7178-T6.

Stress-intensity methods were used to analyze the experimental results. For a given thickness and value of R, the rate of fatigue-crack growth was essentially a single-valued function of the stress-intensity range for 7075-T6 and 7178-T6. An empirical equation developed by Forman, Kearney, and Engle (in Trans. ASME, Ser. D: J. Basic Eng., vol. 89, no. 3, Sept. 1967) fit the 7075-T6 and 7178-T6 crack-growth data reasonably well.

17. Key Words (Suggested by Author(s))	18. Distribution Statement
Fatigue-crack growth Fracture toughness 7075-T6 aluminum alloy 7178-T6 aluminum alloy Thickness effect	Unclassified – Unlimited

19. Security Classif. (of this report)	20. Security Classif. (of this page)	21. No. of Pages	22. Price*
Unclassified	Unclassified	32	$3.00

*For sale by the National Technical Information Service, Springfield, Virginia 22151

EFFECT OF SPECIMEN THICKNESS ON FATIGUE-CRACK-GROWTH BEHAVIOR AND FRACTURE TOUGHNESS OF 7075-T6 AND 7178-T6 ALUMINUM ALLOYS

By C. Michael Hudson and J. C. Newman, Jr.
Langley Research Center

SUMMARY

A study was made to determine the effects of specimen thickness on fatigue-crack growth and fracture behavior of 7075-T6 and 7178-T6 aluminum-alloy sheet and plate. Specimen thicknesses ranged from 5.1 to 12.7 mm (0.20 to 0.50 in.) for 7075-T6 and from 1.3 to 6.4 mm (0.05 to 0.25 in.) for 7178-T6. The stress ratios R used in the crack-growth experiments were 0.02 and 0.50. For 7075-T6, specimen thickness had relatively little effect on fatigue-crack growth. However, the fracture toughness of the thickest gage of 7075-T6 was about two-thirds of the fracture toughness of the thinner gages of 7075-T6. For 7178-T6, fatigue cracks generally grew somewhat faster in the thicker gages than in the thinnest gage. The fracture toughness of the thickest gage of 7178-T6 was about two-thirds of the fracture toughness of the thinner gages of 7178-T6.

Stress-intensity methods were used to analyze the experimental results. For a given thickness and value of R, the rate of fatigue-crack growth was essentially a single-valued function of the stress-intensity range for 7075-T6 and 7178-T6. An empirical equation developed by Forman, Kearney, and Engle (in Trans. ASME, Ser. D: J. Basic Eng., vol. 89, no. 3, Sept. 1967) fit the 7075-T6 and 7178-T6 crack-growth data reasonably well.

INTRODUCTION

Fatigue cracks of various sizes have been discovered during the service life of many aircraft structures. As a result, the predictions of fatigue-crack-growth rates and fracture toughness of parts containing fatigue cracks have become of considerable interest to aircraft designers and operators. In order to make such predictions, the effects of a wide range of parameters must be understood. Many of these parameters, such as component configuration, stress ratio, loading sequence, and environment, have already been investigated at NASA Langley Research Center and are reported in references 1 to 7. However, relatively little research has been conducted on the effects of material thickness on fatigue behavior. Consequently, a series of axial-load fatigue-crack-growth and fracture-toughness experiments were conducted on 7075-T6 and 7178-T6 aluminum-alloy specimens ranging in thickness from 5.1 to 12.7 mm (0.20 to 0.50 in.) and from 1.3 to 6.4 mm (0.05 to 0.25 in.), respectively. These materials were selected because of their frequent use in aircraft construction.

Stress-intensity methods were used to analyze the data because these methods have shown great promise for predicting fatigue-crack propagation and fracture in complex structures. For example, Poe (ref. 8) showed that fatigue-crack growth in stiffened panels can be predicted from stress-intensity parameters and the data from tests of simple sheet specimens.

An empirical equation developed by Forman, Kearney, and Engle (ref. 9) was fitted by least-squares techniques to the fatigue-crack-propagation data. This equation fit the fatigue-crack-growth data generated in a previous study of stress-ratio effects reasonably well (ref. 3).

SYMBOLS

The units used for the physical quantities defined in this paper are given in both the International System of Units (SI) and the U.S. Customary Units. The measurements and calculations were made in the U.S. Customary Units. Factors relating the two systems are given in reference 10 and those used in the present investigation are presented in appendix A.

a	half-length of a central symmetrical crack, mm (in.)
a_i	half-length of crack at start of a fracture-toughness test, mm (in.)
C	constant in fatigue-crack-growth equation
da/dN	rate of fatigue-crack growth, nm/cycle (in./cycle)
E	Young's modulus of elasticity, GN/m^2 (psi)
e	elongation in 51-mm (2-in.) gage length, percent
K_{cn}	critical stress-intensity factor, $\mathrm{MN/m^{3/2}}$ $\left(\mathrm{psi\text{-}in^{1/2}}\right)$
K_{max}	maximum stress-intensity factor, $\mathrm{MN/m^{3/2}}$ $\left(\mathrm{psi\text{-}in^{1/2}}\right)$

K_{min} minimum stress-intensity factor, $MN/m^{3/2}$ $(psi\text{-}in^{1/2})$

ΔK stress-intensity-factor range, $MN/m^{3/2}$ $(psi\text{-}in^{1/2})$

N number of load cycles

n exponent in fatigue-crack-growth equation

P_a amplitude of load applied in a cycle, N (lbf)

P_f maximum load applied to specimen during fracture-toughness test, N (lbf)

P_m mean load applied in a cycle, N (lbf)

P_{max} maximum load applied in a cycle, $P_m + P_a$, N (lbf)

P_{min} minimum load applied in a cycle, $P_m - P_a$, N (lbf)

R ratio of minimum stress to maximum stress

S_a alternating gross stress, P_a/wt, MN/m^2 (psi or ksi)

S_f maximum gross stress applied to specimen during fracture-toughness test, P_f/wt, MN/m^2 (psi)

S_m mean gross stress, P_m/wt, MN/m^2 (psi or ksi)

S_{max} maximum gross stress, P_{max}/wt, MN/m^2 (psi)

S_{min} minimum gross stress, P_{min}/wt, MN/m^2 (psi)

t specimen thickness, mm (in.)

w specimen width, mm (in.)

α secant correction factor for stress intensity in a finite width panel, $\sqrt{\sec \frac{\pi a}{w}}$

σ_u ultimate tensile strength, MN/m^2, (ksi)

σ_y yield strength (0.2-percent offset), MN/m^2 (ksi)

SPECIMENS, TESTS, AND PROCEDURES

Specimens

Through-crack test specimens were made from three thicknesses each of 7075-T6 and 7178-T6 aluminum alloys. The thicknesses and tensile properties of these alloys are listed in table I. The tensile specimens used to obtain these properties met ASTM Standards (ref. 11). The nominal chemical compositions of the two alloys are shown in table II.

The specimen configuration used in both the crack-propagation and fracture-toughness tests is shown in figure 1. These specimens were 292 mm (11.5 in.) wide and 889 mm (35.0 in.) long. The longitudinal axes of all specimens were parallel to the rolling direction of the material. A notch 2.54 mm (0.10 in.) long by 0.25 mm (0.01 in.) wide was cut into the center of each specimen by use of an electrical discharge machining process. The heat-affected zone resulting from this process is less than 0.25 mm (0.01 in.) wide. Consequently, after crack initiation, all of the material through which the fatigue crack propagates is unaltered by the cutting process.

A reference grid (ref. 12) was photographically printed on the surface of the specimen for crack-propagation monitoring. The spacing between grid lines was 1.3 mm (0.050 in.). Metallographic examination and tensile tests conducted on 7075-T6 specimens bearing the grid indicated no detrimental effect on the material.

Testing Machines

Three axial-load fatigue-testing machines were employed in this investigation. The capabilities of these machines are listed in the following table:

Machine type	Maximum load capacity		Operating frequency used		Machine described in –
	kN	lbf	Hz	cpm	
Subresonant	89	20 000	30	1800	Ref. 13
Hydraulic	1334	300 000	1 to 5	60 to 300	App. B
Combination:					
As subresonant unit	467	105 000	14	840	Ref. 14
As hydraulic unit	587	132 000	0.7 to 1.0	40 to 60	

The 1334-kN (300 000-lbf) tester described in the preceding table was also used for fracture-toughness tests requiring loads in excess of 534 kN (120 000 lbf). A hydraulic axial-load universal testing machine was used for fracture-toughness tests requiring lower loads. This universal machine had a load capacity of 534 kN (120 000 lbf).

Test Procedure

Axial-load fatigue-crack-propagation experiments were conducted at stress ratios R of 0.02 and 0.50. The maximum gross stresses in these experiments ranged from 69 to 276 MN/m^2 (10 to 40 ksi) for 7075-T6 and from 52 to 155 MN/m^2 (7.5 to 22.5 ksi) for 7178-T6. The alternating and mean loads were kept constant throughout each test. The fatigue-crack-growth data were obtained by observing crack growth through 10 power microscopes. The number of cycles required to propagate the crack to each grid line was recorded so that crack-propagation rates could be determined.

Fracture-toughness data were obtained two ways. Most of these data came from standard toughness tests in which fatigue-cracked specimens were monotonically loaded to failure at a load rate of 2.2 kN/sec (30 000 lbf/min). The remainder of these data came from fatigue-crack-propagation tests which were continued up to specimen failure. In these tests, the maximum load in the fatigue-crack-propagation test was assumed to be the load at failure.

When a centrally cracked sheet specimen is loaded in axial tension, transverse compressive stresses are generated near the crack surface (ref. 15). These compressive stresses can buckle thin specimens out of the plane of the sheet near the crack. The increase in stress-intensity factor due to this buckling is difficult to calculate; consequently the thinner gage specimens ($t = 5.1$ mm (0.20 in.) for 7075-T6 and $t = 1.3$ and 4.1 mm (0.05 and 0.16 in.) for 7178-T6) were clamped between oiled guide plates (ref. 16) to restrain buckling. The thicker specimens did not buckle; therefore guide plates were not used.

RESULTS AND DISCUSSION

Fatigue-Crack-Growth Experiments

The results of the fatigue-crack-growth experiments on the 7075-T6 and 7178-T6 specimens are presented in table III. This table gives the average number of cycles required for a through-crack to propagate from a half-length of 2.54 mm (0.10 in.) to the listed half-lengths. Fatigue-crack-growth rates were determined graphically from crack-growth curves which were faired through the data of table III.

The fatigue-crack-growth curves for the 7075-T6 specimens of different thicknesses are presented in figure 2. At eight of nine stress levels, fatigue cracks propagated fastest in the 5.1-mm-thick (0.20-in.) 7075-T6 specimens. However, for a given stress level, the ratio of the maximum to the minimum number of cycles required to reach a given crack length never exceeded 1.7, thereby indicating a relatively small thickness effect.

The fatigue-crack-growth curves for the 7178-T6 specimens are presented in figure 3. At six of seven stress levels, fatigue cracks propagated slowest in the 1.3-mm-thick (0.05-in.) 7178-T6 specimens. For a given stress level, the ratio of the maximum to the minimum number of cycles required to reach a given crack length never exceeded 2.7, thereby indicating a moderate thickness effect.

Fatigue-crack-growth curves for 7075-T6 and 7178-T6 specimens of about the same thickness (5.1 and 4.1 mm (0.20 and 0.16 in.), respectively) and tested at the same values of S_{max} and R are shown in figure 4. For a given stress level, the ratio of the maximum to the minimum number of cycles required to reach a given crack length never exceeded 1.7. In two instances fatigue cracks grew fastest in 7075-T6, and in the two other instances, fastest in 7178-T6. Thus, in the thickness range of 4 to 5 mm (0.16 to 0.20 in.), the two alloys appear about equally resistant to fatigue-crack propagation.

Inspection of the fracture surfaces of the specimens (fig. 5, for example) indicated that intermittent bursts of crack growth (referred to hereinafter as "pop-in" (ref. 17)) occurred in the interior of specimens having thicknesses as small as 4.1 mm (0.16 in.). The dark areas in figure 5 indicate pop-in. The light areas indicate normal, microscopic fatigue-crack growth. The reason for this pop-in is not understood at this time.

The fatigue-crack-growth data in table III were analyzed by using stress-intensity methods (see appendix C). For a given thickness and value of R, the rate of fatigue-crack growth was a single-valued function of the stress-intensity range for 7075-T6 and 7178-T6 (fig. 6).

An empirical fatigue-crack-growth equation developed by Forman, Kearney, and Engle (ref. 9) was fitted to the test data. This equation has the form

$$\frac{da}{dN} = \frac{C(\Delta K)^n}{(1 - R)K_{cn} - \Delta K} \qquad (1)$$

(The symbol K_{cn} is denoted by K_c in ref. 9.)

The empirical constants C and n were determined by using least-squares techniques to fit the equation to the data. When these constants were determined in SI Units, ΔK and K_{cn} were given in $MN/m^{3/2}$ and da/dN was given in nm/cycle. When C and n were computed in U.S. Customary Units, ΔK and K_{cn} were given in psi-in$^{1/2}$ and da/dN was given in in./cycle. The values of C and n determined for the different thicknesses are listed in the following table:

Aluminum alloy	t		C		n
	mm	in.	SI Units	U.S. Customary Units	
7075-T6	5.1	0.20	25.9	1.05×10^{-11}	2.69
	9.7	.38	23.1	1.19×10^{-11}	2.63
	12.7	.50	58.2	2.77×10^{-9}	1.99
7178-T6	1.3	0.05	18.5	3.63×10^{-11}	2.45
	4.1	.16	23.8	2.96×10^{-11}	2.52
	6.4	.25	63.2	1.80×10^{-8}	1.72

Equation (1) fit the test data reasonably well.

Fracture-Toughness Experiments

The results of the fracture-toughness experiments on the 7075-T6 and 7178-T6 specimens are listed in table IV. This table gives the half-length of the crack at the start of the fracture-toughness test a_i, the maximum gross stress applied to the test specimen during the fracture-toughness test S_f, and the critical stress-intensity factor K_{cn}. This factor was calculated by using the equation

$$K_{cn} = \left(\frac{P_f}{wt}\right)\sqrt{a_i \pi \alpha} \tag{2}$$

where α is given in appendix C.

The values of K_{cn} for the various thicknesses are plotted against a_i in figure 7. Analysis of the data in figure 7 indicates that the fracture toughness of the 12.7-mm-thick (0.50-in.) 7075-T6 was, on the average, about two-thirds of the fracture toughness of the thinner gages of 7075-T6. The average fracture toughness of the 6.4-mm-thick (0.25-in.) 7178-T6 was about two-thirds of the fracture toughness of the thinner gages of 7178-T6. Figure 7 also indicates that K_{cn} increased with increasing crack length. A similar variation of K_{cn} with crack length occurred in tests on through-cracked 2014-T6 and 2219-T87 aluminum alloys (ref. 18).

Values of K_{cn} for 7075-T6 and 7178-T6 specimens of about the same thickness (5.1 and 4.1 mm (0.20 and 0.16 in.)) are plotted against a_i in figure 8. The fracture toughness of 7075-T6 was about 20 percent higher than the fracture toughness of 7178-T6.

CONCLUSIONS

A study was made to determine the effects of specimen thickness on fatigue-crack growth and fracture behavior of 7075-T6 and 7178-T6 aluminum-alloy sheet and plate.

The 7075-T6 specimens had thicknesses of 5.1, 9.7, and 12.7 mm (0.20, 0.38, and 0.50 in.); the 7178-T6 specimens had thicknesses of 1.3, 4.1, and 6.4 mm (0.05, 0.16, and 0.25 in.). The stress ratios R (ratio of the minimum stress to the maximum stress) used in these experiments were 0.02 and 0.50. The experimental results were analyzed by using stress-intensity methods, and an empirical equation was fitted to the data. The following conclusions can be drawn from this study:

1. For 7075-T6, material thickness had relatively little effect on fatigue-crack growth. The fracture toughness of the 12.7-mm-thick (0.50-in.) 7075-T6 was about two-thirds of the fracture toughness of the thinner gages of 7075-T6.

2. For 7178-T6, fatigue cracks generally grew somewhat faster in the thicker gages than in the thinnest gage. The fracture toughness of the 6.4-mm-thick (0.25-in.) 7178-T6 was about two-thirds of the fracture toughness of the thinner gages of 7178-T6.

3. For a nominal thickness of 5.1 mm (0.20 in.), fatigue cracks in 7075-T6 and 7178-T6 propagated to a given crack length in approximately the same number of cycles. For the same nominal thickness, the fracture toughness of 7075-T6 was about 20 percent higher than the fracture toughness of 7178-T6.

4. During the fatigue-crack-growth tests, intermittent bursts of crack growth (pop-in) occurred in the interior of the 7075-T6 and 7178-T6 specimens having thicknesses $\geqq$4.1 mm (0.16 in.). The reason for this pop-in is not understood at present.

5. An empirical equation developed by Forman, Kearney, and Engle (in Trans. ASME, Ser. D: J. Basic Eng., vol. 89, no. 3, Sept. 1967) fit both the 7075-T6 and 7178-T6 crack-growth data reasonably well.

6. For a given thickness and value of R, the rate of fatigue-crack growth was essentially a single-valued function of the stress-intensity range for 7075-T6 and 7178-T6.

Langley Research Center,
National Aeronautics and Space Administration,
Hampton, Va., February 20, 1973.

APPENDIX A

CONVERSION OF SI UNITS TO U.S. CUSTOMARY UNITS

The International System of Units (SI) was adopted by the Eleventh General Conference on Weights and Measures held in Paris in 1960 (ref. 10). Conversion factors required for units used herein are given in the following table:

Physical quantity	SI Unit (a)	Conversion factor (b)	U.S. Customary Unit
Force	newtons (N)	0.2248	lbf
Length	meters (m)	$.3937 \times 10^2$	in.
Stress	newtons per sq meter (N/m^2)	$.145 \times 10^{-6}$	ksi = 10^3 lbf/in^2
Stress intensity	newtons per meter$^{3/2}$ $\left(N/m^{3/2}\right)$	$.9099 \times 10^{-6}$	ksi-in$^{1/2}$
Frequency	hertz (Hz)	60	cpm

[a]Prefixes and symbols to indicate multiples of units are as follows:

Multiple	Prefix	Symbol
10^{-9}	nano	n
10^{-3}	milli	m
10^3	kilo	k
10^6	mega	M
10^9	giga	G

[b]Multiply value given in SI Unit by conversion factor to obtain equivalent in U.S Customary Unit.

APPENDIX B

DESCRIPTION OF 1334-kN (300 000-lbf) FATIGUE TESTER

The 1334-kN (300 000-lbf) machine is an analog closed-loop servohydraulic fatigue-testing system. A schematic diagram of the loading system is shown in figure 9. To use this system, the operator first sets in the desired mean load by adjusting the mean-load potentiometer. Then the desired alternating load is set by adjusting the alternating-load potentiometer (which controls the amplitude of the function generator signal).

The voltages from the mean-load potentiometer and the function generator are combined to form a command signal which is fed into the servoloop summing point. The voltage from a transducer – either the load cell or the linearly variable displacement transformer (LVDT) – is also fed into this summing point. The command and transducer voltages are summed and suitably amplified to form a signal which drives the servovalve. This servovalve directs oil to the appropriate side of the hydraulic cylinder to obtain the commanded load. Load repeatability for this testing system is ±0.5 percent of the applied load.

Loads are monitored by comparing on an oscilloscope the output voltage from the load cell (or LVDT) with an adjustable bias voltage which corresponds to the desired load level for the test. When the sum of these voltages is zero, the desired load is on the test specimen. (This comparison is made at both the maximum and minimum loads in the cycle.) The accuracy of this monitoring system is better than ±0.1 percent of full scale.

APPENDIX C

FATIGUE-CRACK-GROWTH ANALYSIS

The fatigue-crack-growth data were correlated by the stress-intensity methods. Paris (ref. 19) hypothesized that the rate of fatigue-crack growth was a function of the stress-intensity range; that is

$$\frac{da}{dN} = f(\Delta K) \tag{C1}$$

where

$$\Delta K = K_{max} - K_{min} \tag{C2}$$

For centrally cracked specimens subjected to a uniformly distributed axial load

$$K_{max} = \alpha S_{max} \sqrt{a\pi} \tag{C3}$$

and

$$K_{min} = \alpha S_{min} \sqrt{a\pi} \tag{C4}$$

The term α is a factor intended to correct for the finite width of the specimen (ref. 20) and is given by

$$\alpha = \sqrt{\sec \frac{\pi a}{w}} \tag{C5}$$

REFERENCES

1. Hudson, C. Michael: Investigation of Fatigue Crack Growth in Ti-8Al-1Mo-1V (Duplex-Annealed) Specimens Having Various Widths. NASA TN D-3879, 1967.

2. Figge, I. E.: Residual-Static-Strength and Slow-Crack-Growth Behavior of Duplex-Annealed Ti-8Al-1Mo-1V Sheet. NASA TN D-4358, 1968.

3. Hudson, C. Michael: Effect of Stress Ratio on Fatigue-Crack Growth in 7075-T6 and 2024-T3 Aluminum-Alloy Specimens. NASA TN D-5390, 1969.

4. Hudson, C. Michael; and Hardrath, Herbert F.: Effects of Changing Stress Amplitude on the Rate of Fatigue-Crack Propagation in Two Aluminum Alloys. NASA TN D-960, 1961.

5. Hudson, C. Michael; and Raju, K. N.: Investigation of Fatigue-Crack Growth Under Simple Variable-Amplitude Loading. NASA TN D-5702, 1970.

6. Figge, I. E.; and Hudson, C. Michael: Crack Propagation, Delayed Failure, and Residual Static Strength of Titanium, Aluminum, and Stainless Steel Alloys in Aqueous Environments. NASA TN D-3825, 1967.

7. Figge, I. E.; and Newman, J. C., Jr.: Fatigue Crack Propagation in Structures With Simulated Rivet Forces. Fatigue Crack Propagation, Spec. Tech. Publ. No. 415, Amer. Soc. Testing Mater., 1967, pp. 71-93.

8. Poe, C. C., Jr.: Fatigue Crack Propagation in Stiffened Panels. Damage Tolerance in Aircraft Structures, Spec. Tech. Publ. No. 486, Amer. Soc. Testing Mater., 1971, pp. 79-97.

9. Forman, R. G.; Kearney, V. E.; and Engle, R. M.: Numerical Analysis of Crack Propagation in Cyclic-Loaded Structures. Trans. ASME, Ser. D: J. Basic Eng., vol. 89, no. 3, Sept. 1967, pp. 459-464.

10. Comm. on Metric Pract.: ASTM Metric Practice Guide. NBS Handbook 102, U.S. Dep. Com., Mar. 10, 1967.

11. Anon.: Standard Methods of Tension Testing of Metallic Materials. ASTM Designation: E 8-69. Pt. 31 of 1971 Annual Book of ASTM Standards. Amer. Soc. Testing Mater., c.1971, pp. 194-213.

12. Hudson, C. Michael: Fatigue-Crack Propagation in Several Titanium and Stainless-Steel Alloys and One Superalloy. NASA TN D-2331, 1964.

13. Grover, H. J.; Hyler, W. S.; Kuhn, Paul; Landers, Charles B.; and Howell, F. M.: Axial-Load Fatigue Properties of 24S-T and 75S-T Aluminum Alloy as Determined in Several Laboratories. NACA Rep. 1190, 1954. (Supersedes NACA TN 2928.)

14. Hudson, C. Michael; and Hardrath, Herbert F.: Investigation of the Effects of Variable-Amplitude Loadings on Fatigue Crack Propagation Patterns. NASA TN D-1803, 1963.

15. Kuhn, Paul; and Figge, I. E.: Unified Notch-Strength Analysis for Wrought Aluminum Alloys. NASA TN D-1259, 1962.

16. Brueggeman, W. C.; and Mayer, M., Jr.: Guides for Preventing Buckling in Axial Fatigue Tests of Thin Sheet-Metal Specimens. NACA TN 931, 1944.

17. Hartbower, C. E.; Gerberich, W. W.; and Liebowitz, H.: Investigation of Crack-Growth Stress-Wave Relationships. Eng. Fracture Mech., vol. 1, no. 2, Aug. 1968, pp. 291-308.

18. Orange, Thomas W.; Sullivan, Timothy L.; and Calfo, Frederick D.: Fracture of Thin Sections Containing Through and Part-Through Cracks. NASA TN D-6305, 1971.

19. Paris, Paul C.: The Fracture Mechanics Approach to Fatigue. Fatigue – An Interdisciplinary Approach, John J. Burke, Norman L. Reed, and Volker Weiss, eds., Syracuse Univ. Press, 1964, pp. 107-132.

20. Brown, William F.; and Srawley, John E.: Plane Strain Crack Toughness Testing of High Strength Metallic Materials. Spec. Tech. Publ. No. 410, Amer. Soc. Testing Mater., c.1966.

TABLE I.- AVERAGE TENSILE PROPERTIES OF ALUMINUM ALLOYS TESTED

t		σ_u		σ_y		e, %	E		No. of tests
mm	in.	MN/m^2	ksi	MN/m^2	ksi		GN/m^2	psi	
7075-T6									
5.1	0.20	595	86.3	542	78.6	13.0	69.0	10.0×10^6	6
9.7	.38	574	83.3	528	76.6	12.6	69.7	10.1	6
12.7	.50	598	86.7	551	79.9	15.5	69.7	10.1	6
7178-T6									
1.3	0.05	608	88.2	564	81.8	12.7	66.9	9.7×10^6	3
4.1	.16	624	90.5	586	85.0	12.8	69.0	10.0	6
6.4	.25	622	90.2	593	86.0	13.0	69.7	10.1	6

TABLE II.- NOMINAL CHEMICAL COMPOSITIONS OF ALUMINUM ALLOYS TESTED

Aluminum alloy	t		Element, percent by weight									
	mm	in.	Si	Fe	Cu	Mn	Mg	Ni	Cr	Zn	Ti	Al
7075-T6	5.1	0.20	0.11	0.28	1.72	0.13	2.74	0.01	0.21	5.63	0.05	Bal.
	9.7	.38	.11	.25	1.69	.07	2.51	.02	.20	5.70	.05	Bal.
	12.7	.50	.11	.28	1.72	.13	2.74	.01	.21	5.63	.05	Bal.
7178-T6	1.3	0.05	0.11	0.28	1.76	0.05	2.64	0.02	0.19	6.97	0.04	Bal.
	4.1	.16	.08	.28	2.06	.07	2.99	.02	.20	6.86	.03	Bal.
	6.4	.25	.08	.28	2.06	.07	2.99	.02	.20	6.86	.03	Bal.

TABLE III.- AVERAGE NUMBER OF CYCLES REQUIRED TO EXTEND CRACKS FROM A HALF-LENGTH OF 2.54 mm (0.10 in.) TO VARIOUS LENGTHS

(a) 7075-T6

t		S_m		S_a		Loading frequency		R	Average number of cycles required to propagate a crack from a half-length a of[a] 2.54 mm (0.10 in.) to a half-length a of –													
mm	in.	MN/m^2	ksi	MN/m^2	ksi	Hz	cpm		3.81 mm (0.15 in.)	5.08 mm (0.20 in.)	7.62 mm (0.30 in.)	10.16 mm (0.40 in.)	12.70 mm (0.50 in.)	15.24 mm (0.60 in.)	17.78 mm (0.70 in.)	20.32 mm (0.80 in.)	22.86 mm (0.90 in.)	25.40 mm (1.00 in.)	30.48 mm (1.20 in.)	35.56 mm (1.40 in.)	40.64 mm (1.60 in.)	45.72 mm (1.80 in.)
		140.7	20.40	135.1	19.60	1.0	60	0.02	236	346												
		105.5	15.30	101.4	14.70	1.0	60	.02	535	805	1 095	1 190	1 220									
		70.3	10.20	67.6	9.80	1.0	60	.02	1 600	2 520	3 660	4 360	4 780	5 080	5 280	5 400	5 480	5 520				
		52.7	7.65	50.7	7.35	1.0	60	.02	2 800	4 750	7 500	9 200	10 550	11 650	12 600	13 200	13 750	14 150	14 650	14 950	15 100	
5.1	0.20	35.2	5.10	33.8	[b]4.90	3.0	180	.02			6 000	11 000	14 800	17 900	20 500	22 600	24 500	26 100	28 800	31 000	32 700	33 900
		206.9	30.00	69.0	10.00	1.0	60	.50	530	675	785	820										
		172.4	25.00	57.2	8.30	1.0	60	.50	1 000	1 460	1 790	1 900	1 960									
		137.9	20.00	46.2	6.70	1.0	60	.50	3 100	4 300	5 600	6 100	6 350	6 500	6 575	6 625						
		103.4	15.00	34.5	5.00	1.0	60	.50	4 600	8 000	11 700	13 600	14 800	15 600	16 000	16 400	16 600	16 700				
		68.8	9.975	22.9	[c]3.325	3.0	180	.50			12 200	20 400	26 000	30 200	33 000	35 000	36 600	37 800	39 400	40 600	41 200	41 600
		140.7	20.40	135.1	19.60	1.0	60	0.02	327	492												
		105.5	15.30	101.4	14.70	1.0	60	.02	705	1 050	1 430	1 560										
		70.3	10.20	67.6	9.80	1.0	60	.02	2 200	3 720	5 360	6 340	7 020	7 520	7 860	8 080	8 250	8 360	8 490			
		52.7	7.65	50.7	7.35	1.0	60	.02	5 200	8 300	12 600	15 500	17 400	18 800	19 800	20 600	21 200	21 700	22 400	22 900	23 200	23 400
9.7	0.38	172.4	25.00	57.2	8.30	1.0	60	.50	1 270	1 810	2 160	2 290	2 355									
		137.9	20.00	46.2	6.70	1.0	60	.50	3 650	5 650	7 450	8 150	8 550	8 650	8 750							
		103.4	15.00	34.5	5.00	1.0	60	.50	6 100	11 100	19 100	23 100	25 100	26 100	26 800	27 200	27 450	27 700	27 900	28 100		
		68.8	9.975	22.9	3.325	1.0	60	.50	52 000	77 000	99 000	110 000	118 000	123 000	127 500	130 000	131 750	133 000	135 000	136 700	137 800	138 300
		105.5	15.30	101.4	14.70	1.0	60	0.02	690	1 140	1 565											
		70.3	10.20	67.6	9.80	1.0	60	.02	2 475	4 300	6 550	7 650	8 075									
		52.7	7.65	50.7	7.35	1.0	60	.02	5 600	8 725	12 400	15 000	16 800	18 100	19 000	19 600	19 900					
12.7	0.50	35.2	5.10	33.8	[b]4.90	1.0	60	.02			9 650	15 250	19 250	22 400	25 250	27 650	29 650	31 250	34 150	36 250	37 750	38 650
		172.4	25.00	57.2	8.30	1.0	60	.50	1 965													
		137.9	20.00	46.2	6.70	1.0	60	.50	3 625	5 150												
		103.4	15.00	34.5	5.00	1.0	60	.50	5 450	9 700	14 800	16 900	17 500	17 650								
		68.8	9.975	22.9	3.325	1.0	60	.50	13 000	22 500	35 350	42 700	47 700	51 500	54 350	56 350	57 700	58 700	59 600			

[a]Except as noted.

[b]Crack was initiated and propagated to a = 3.81 mm (0.15 in.) at S_{max} = 96.53 MN/m^2 (14 ksi) to expedite testing; cycles listed are number required to propagate crack from a = 5.08 mm (0.20 in.).

[c]Crack was initiated and propagated to a = 3.81 mm (0.15 in.) at S_{max} = 103.42 MN/m^2 (15 ksi) to expedite testing; cycles listed are number required to propagate crack from a = 5.08 mm (0.20 in.).

TABLE III.- AVERAGE NUMBER OF CYCLES REQUIRED TO EXTEND CRACKS FROM A HALF-LENGTH OF 2.54 mm (0.10 in.) TO VARIOUS LENGTHS – Concluded

(b) 7178-T6

t		S_m		S_a		Loading frequency		R	Average number of cycles required to propagate a crack from a half-length a of[a] 2.54 mm (0.10 in.) to a half-length a of –													
mm	in.	MN/m²	ksi	MN/m²	ksi	Hz	cpm		3.81 mm (0.15 in.)	5.08 mm (0.20 in.)	7.62 mm (0.30 in.)	10.16 mm (0.40 in.)	12.70 mm (0.50 in.)	15.24 mm (0.60 in.)	17.78 mm (0.70 in.)	20.32 mm (0.80 in.)	22.86 mm (0.90 in.)	25.40 mm (1.00 in.)	30.48 mm (1.20 in.)	35.56 mm (1.40 in.)	40.64 mm (1.60 in.)	45.72 mm (1.80 in.)
		70.3	10.20	67.6	9.80	1.0	60	0.02	3 150	5 075	7 200	8 225	8 800	9 125	9 350	9 500						
		52.7	7.65	50.7	7.35	1.0	60	.02	10 100	15 000	21 200	25 000	27 100	28 500	29 500	30 200						
		35.2	5.10	33.8	4.90	14.0	840	.02	54 000	74 000	90 500	101 000	110 000	117 500	123 500	128 000	131 500	134 500	139 000	141 500		
1.3	0.05	26.4	3.825	25.3	[b]3.675	14.0	840	.02			43 000	67 000	83 000	94 000	104 000	110 000	116 000	122 000	131 000			
		103.4	15.00	34.5	5.00	1.0	60	.50	4 800	7 900	11 400	13 450	14 700	15 700	16 400	16 900						
		77.6	11.25	25.9	3.75	1.0	60	.50	12 250	18 500	27 375	33 000	37 250	40 625	43 500	45 750						
		51.7	7.50	17.2	[c]2.50	14.0	840	.50			63 000	97 000	119 000	135 000	146 000	153 000	159 000	164 000	171 000	177 000	181 000	
		70.3	10.20	67.6	9.80	1.0	60	0.02	1 300	2 160	3 100	3 600	3 880	4 040	4 140	4 190	4 220					
		52.7	7.65	50.7	7.35	14.0	840	.02	4 000	7 100	12 100	15 350	17 400	18 700	19 450	19 800						
		35.2	5.10	33.8	4.90	14.0	840	.02	20 000	31 000	43 500	51 000	56 500	61 000	65 000	68 000	70 500	72 500	75 500			
4.1	0.16	26.4	3.825	25.3	[b]3.675	14.0	840	.02			28 500	45 000	56 000	64 000	71 500	78 500	84 000	89 000	98 000	104 500	110 000	113 500
		103.4	15.00	34.5	5.00	3.0	180	.50	4 000	6 200	8 800	9 950	10 550	10 950	11 150	11 300	11 350	11 400				
		77.6	11.25	25.9	3.75	14.0	840	.50	12 400	18 800	25 900	30 500	33 200	35 000	36 100							
		51.7	7.50	17.2	[c]2.50	3.0	180	.50			39 000	55 500	67 000	75 500	82 000	86 500	90 000	93 000	97 500	101 500	103 500	105 500
		79.1	11.475	76.0	11.025	1.0	60	0.02	2 110	3 350												
		70.3	10.20	67.6	9.80	1.0	60	.02	2 250	4 150	6 100	6 725										
		52.7	7.65	50.7	7.35	1.5	90	.02	4 300	7 500	11 650	14 200	15 800									
6.4	0.25	35.2	5.10	33.8	4.90	13.0	780	.02	24 500	37 000	53 500	64 000	71 000	76 500	81 000	84 750	87 750	90 000	92 500			
		26.4	3.825	25.3	[b]3.675	5.0	300	.02			21 000	35 000	45 500	54 500	62 000	68 000	73 000	77 250	84 500	90 500	95 000	
		103.4	15.00	34.5	5.00	1.0	60	.50	7 400	12 100	15 900											
		77.6	11.25	25.9	3.75	2.0	120	.50	8 000	14 500	25 250	32 000										
		51.7	7.50	17.2	[c]2.50	10.0	600	.50			14 000	26 500	36 500	44 750	51 250	57 250						

[a]Except as noted.

[b]Crack was initiated and propagated to a = 3.05 mm (0.12 in.) at S_{max} = 68.95 MN/m² (10 ksi) to expedite testing; cycles listed are number required to propagate crack from a = 5.08 mm (0.20 in.).

[c]Crack was initiated and propagated to a = 3.05 mm (0.12 in.) at S_{max} = 86.18 MN/m² (12 ksi) to expedite testing; cycles listed are number required to propagate crack from a = 5.08 mm (0.20 in.).

TABLE IV.- VALUES OF K_{cn} FROM FRACTURE-TOUGHNESS TESTS

(a) 7075-T6

t		a_i		S_f		K_{cn}	
mm	in.	mm	in.	MN/m^2	psi	$MN/m^{3/2}$	psi-$in^{1/2}$
[a]5.1	0.20	6.6	0.26	294	42.7×10^3	42.2	38.4×10^3
		10.2	.40	268	38.9	47.9	43.5
		18.5	.73	211	30.6	51.4	46.7
		22.1	.87	185	26.9	49.2	44.8
		27.2	1.07	161	23.3	47.7	43.4
		35.6	1.40	152	22.0	52.8	48.0
		49.5	1.95	125	18.0	52.9	48.1
		61.5	2.42	103	15.0	51.4	46.7
		78.0	3.07	88	12.7	53.0	48.2
9.7	0.38	5.1	0.20	297	43.1×10^3	37.4	34.0×10^3
		6.4	.25	306	44.4	43.0	39.1
		7.9	.31	291	42.2	46.0	41.8
		9.1	.36	276	40.0	46.2	42.0
		11.4	.45	248	35.9	47.0	42.8
		15.0	.59	243	35.2	53.1	48.3
		20.3	.80	218	31.6	55.8	50.8
		29.7	1.17	179	26.0	56.5	51.4
		37.8	1.49	155	22.5	55.6	50.6
		53.6	2.11	133	19.3	59.3	53.9
		62.2	2.45	114	16.5	56.6	51.5
		78.0	3.07	101	14.7	61.3	55.7
12.7	0.50	4.8	0.19	230	33.3×10^3	28.2	25.6×10^3
		6.9	.27	207	30.0	30.3	27.6
		9.1	.36	184	26.7	31.1	28.3
		13.5	.53	154	22.4	32.0	29.1
		15.0	.59	154	22.3	33.7	30.7
		22.4	.88	123	17.8	32.8	29.9
		32.5	1.28	111	16.1	36.7	33.4
		48.5	1.91	90	13.0	37.6	34.2

[a]Guide plates used.

TABLE IV.- VALUES OF K_{cn} FROM FRACTURE-TOUGHNESS TESTS – Concluded

(b) 7178-T6

t		a_i		S_f		K_{cn}	
mm	in.	mm	in.	MN/m^2	psi	MN/m$^{3/2}$	psi-in$^{1/2}$
[a]1.3	0.05	23.6	0.93	153	22.2×10^3	42.5	38.6×10^3
		24.9	.98	140	20.3	39.7	36.2
		33.8	1.33	124	18.0	41.5	37.8
		44.2	1.74	103	14.9	40.7	37.1
		47.5	1.87	99	14.4	40.9	37.2
[a]4.1	0.16	17.8	0.70	156	22.6×10^3	37.2	33.9×10^3
		21.3	.84	152	22.1	39.7	36.1
		25.9	1.02	139	20.2	40.6	36.9
		40.1	1.58	112	16.2	41.7	37.9
		56.6	2.23	91	13.2	42.3	38.5
6.4	0.25	7.6	0.30	157	22.8×10^3	24.3	22.1×10^3
		13.5	.53	128	18.5	26.5	24.1
		13.7	.54	122	17.7	25.5	23.2
		15.5	.61	122	17.7	27.1	24.6
		23.9	.94	98	14.2	27.4	24.9
		35.3	1.39	79	11.4	27.3	24.9
		46.7	1.84	75	10.9	30.8	28.0

[a]Guide plates used.

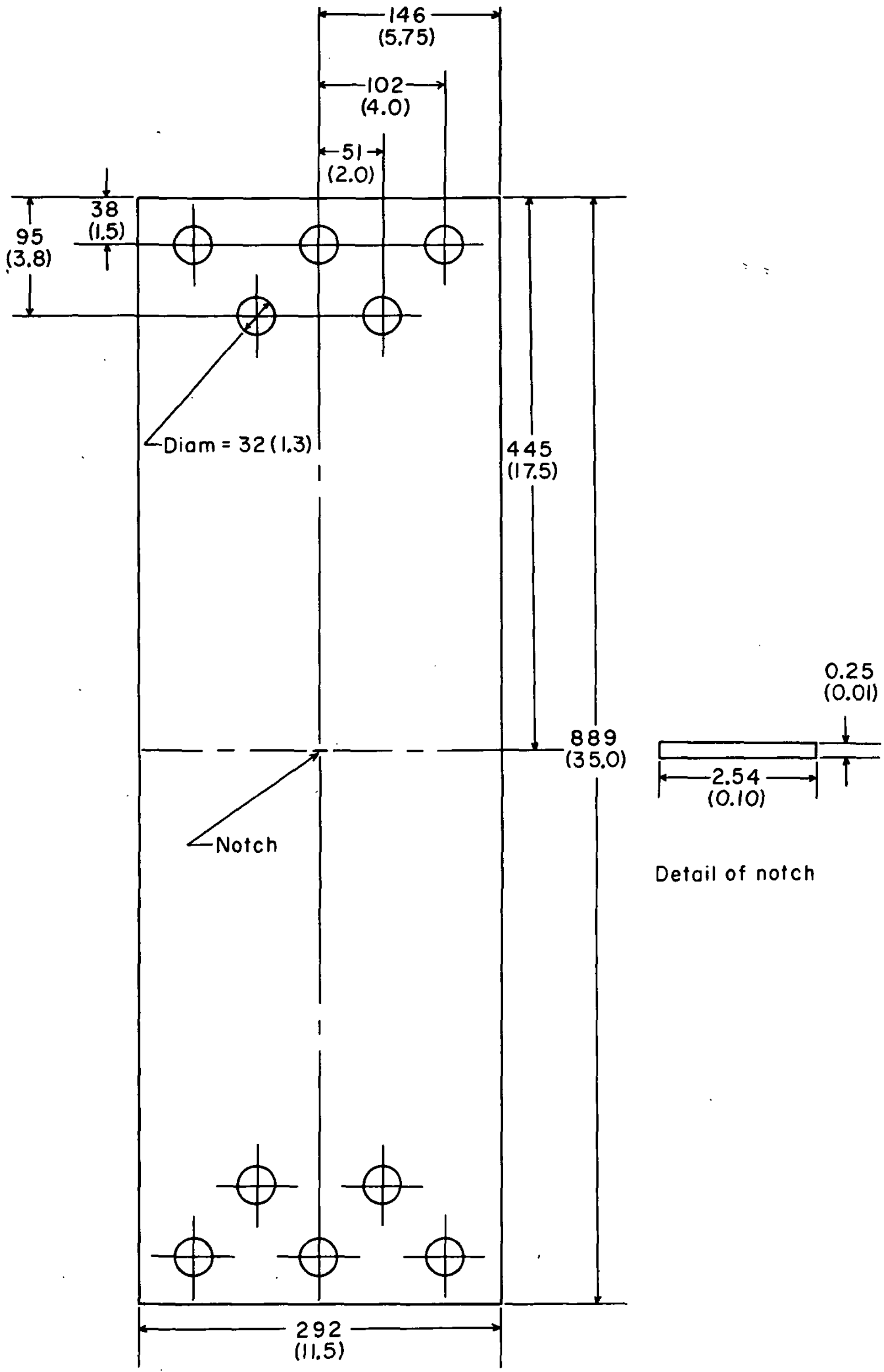

Figure 1.- Specimen configuration. All dimensions in mm (in.).

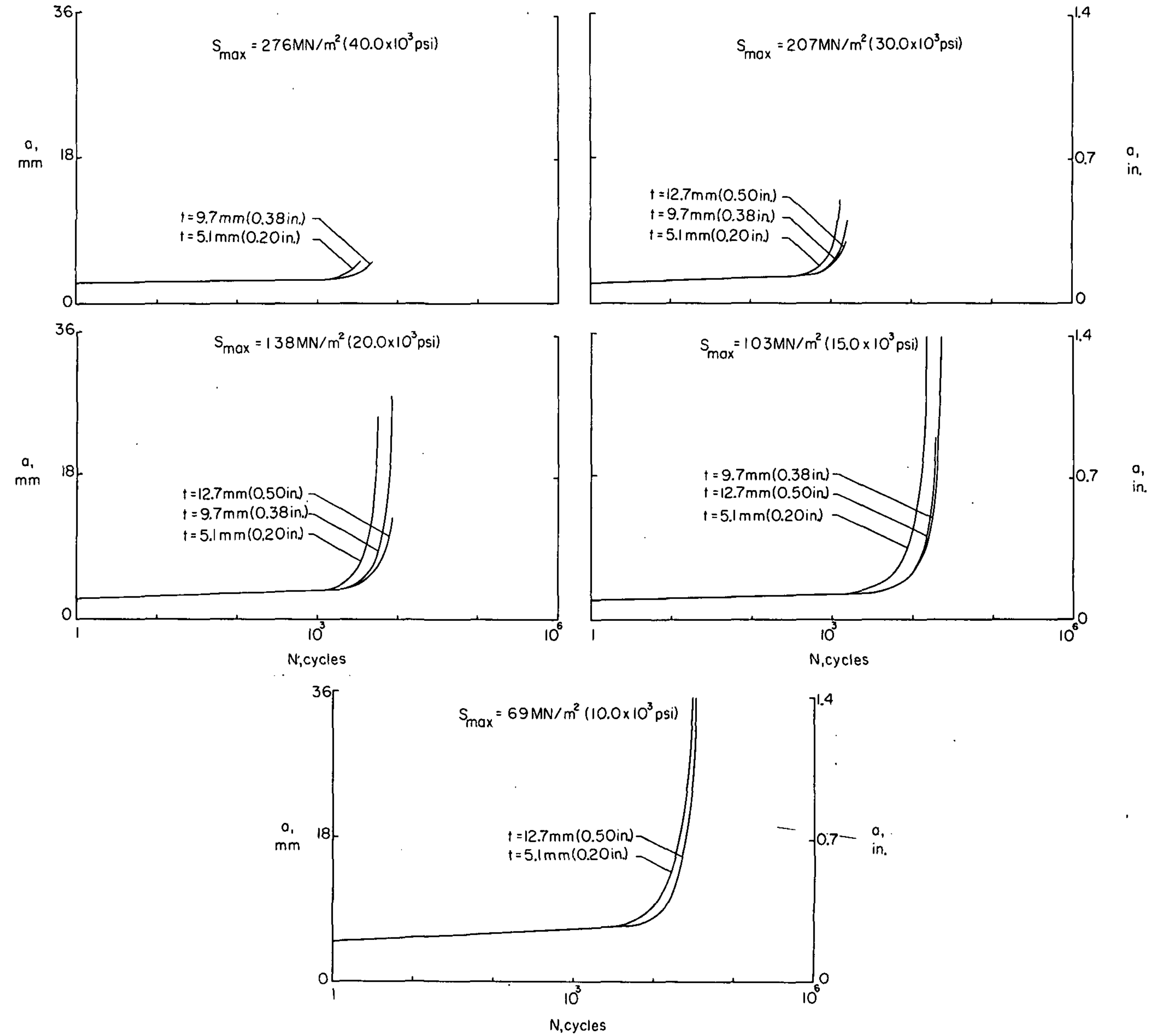

(a) R = 0.02.

Figure 2.- Fatigue-crack-growth curves for 7075-T6 specimens having different thicknesses.

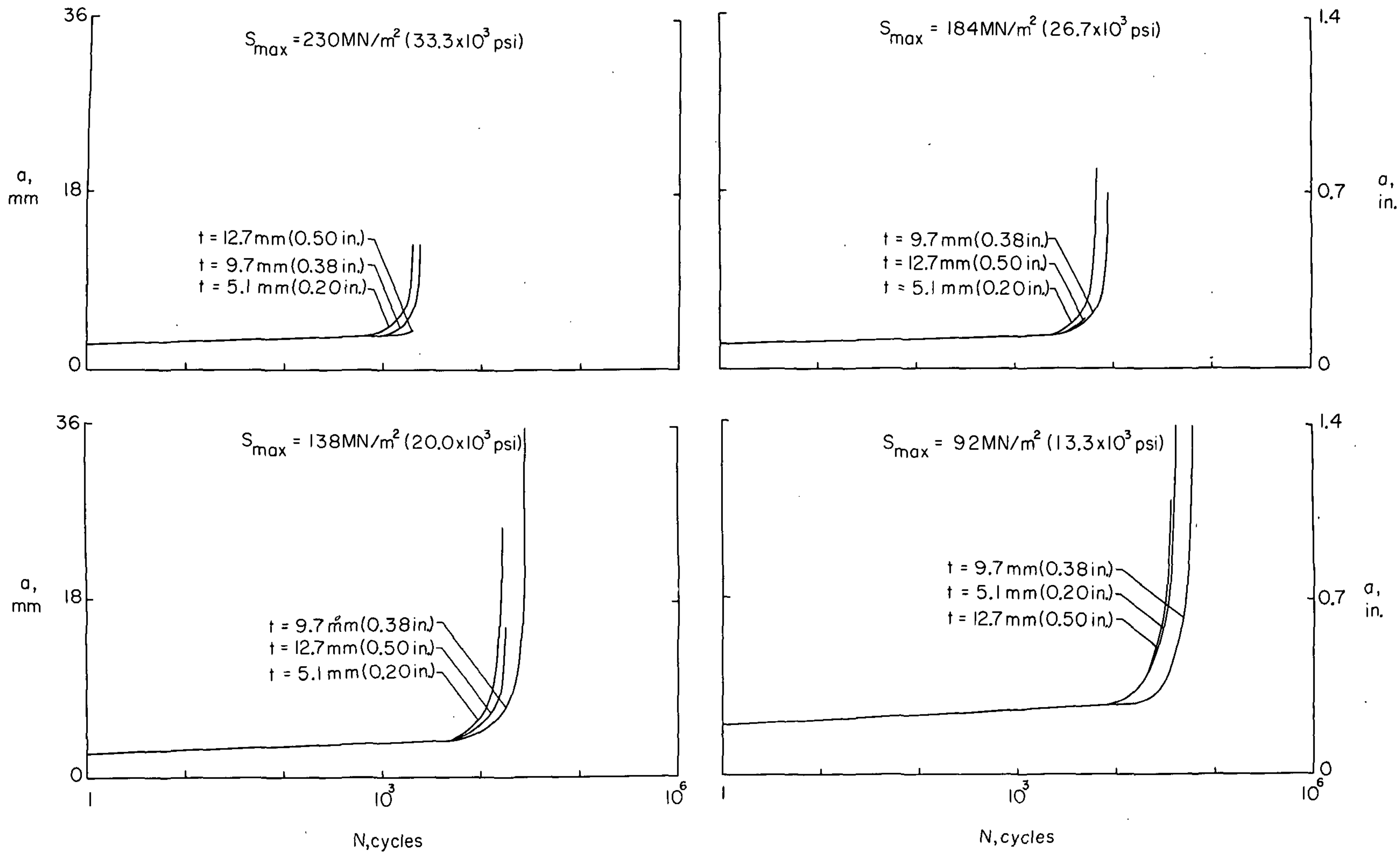

(b) R = 0.50.

Figure 2.- Concluded.

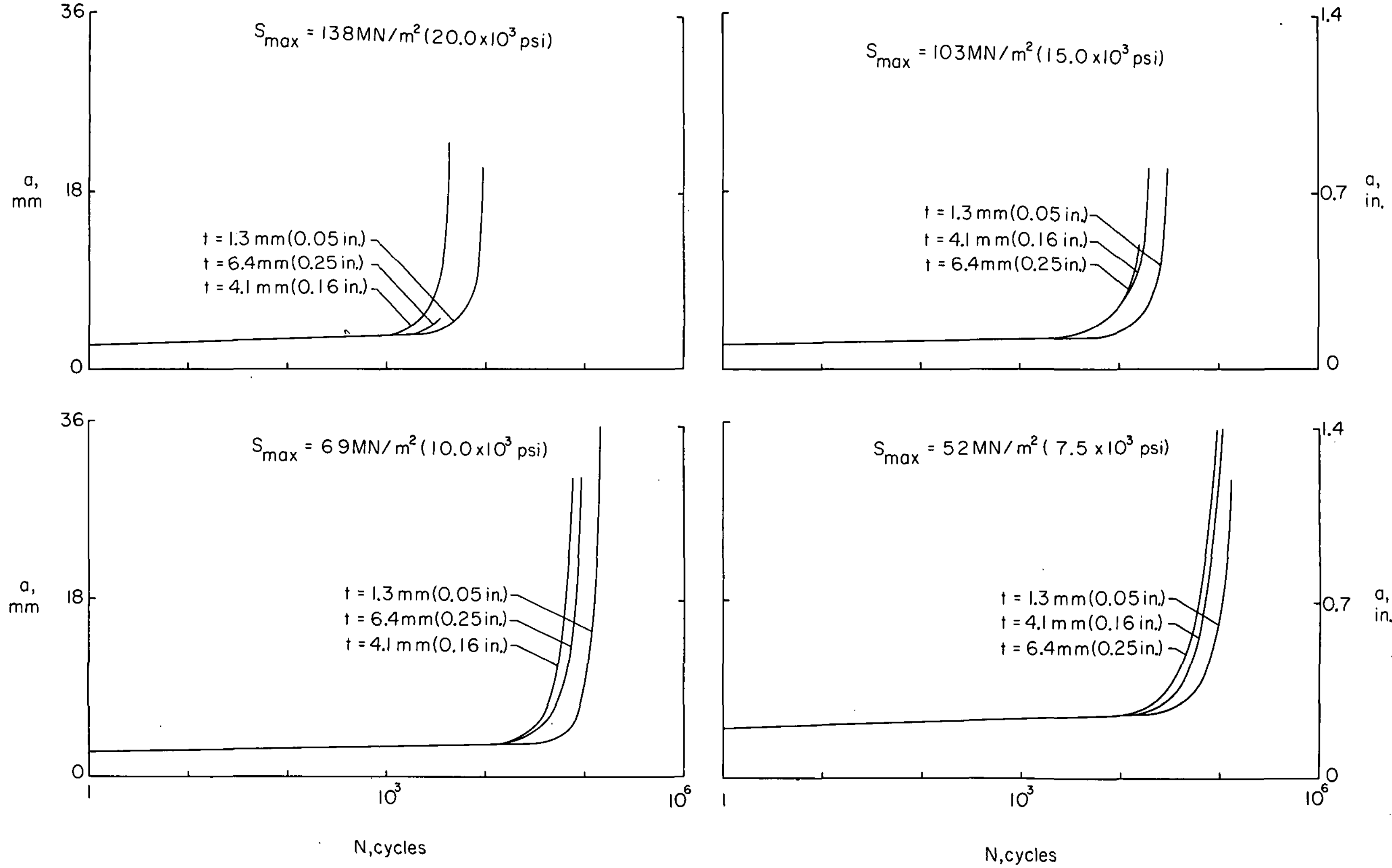

(a) R = 0.02.

Figure 3.- Fatigue-crack-growth curves for 7178-T6 specimens having different thicknesses.

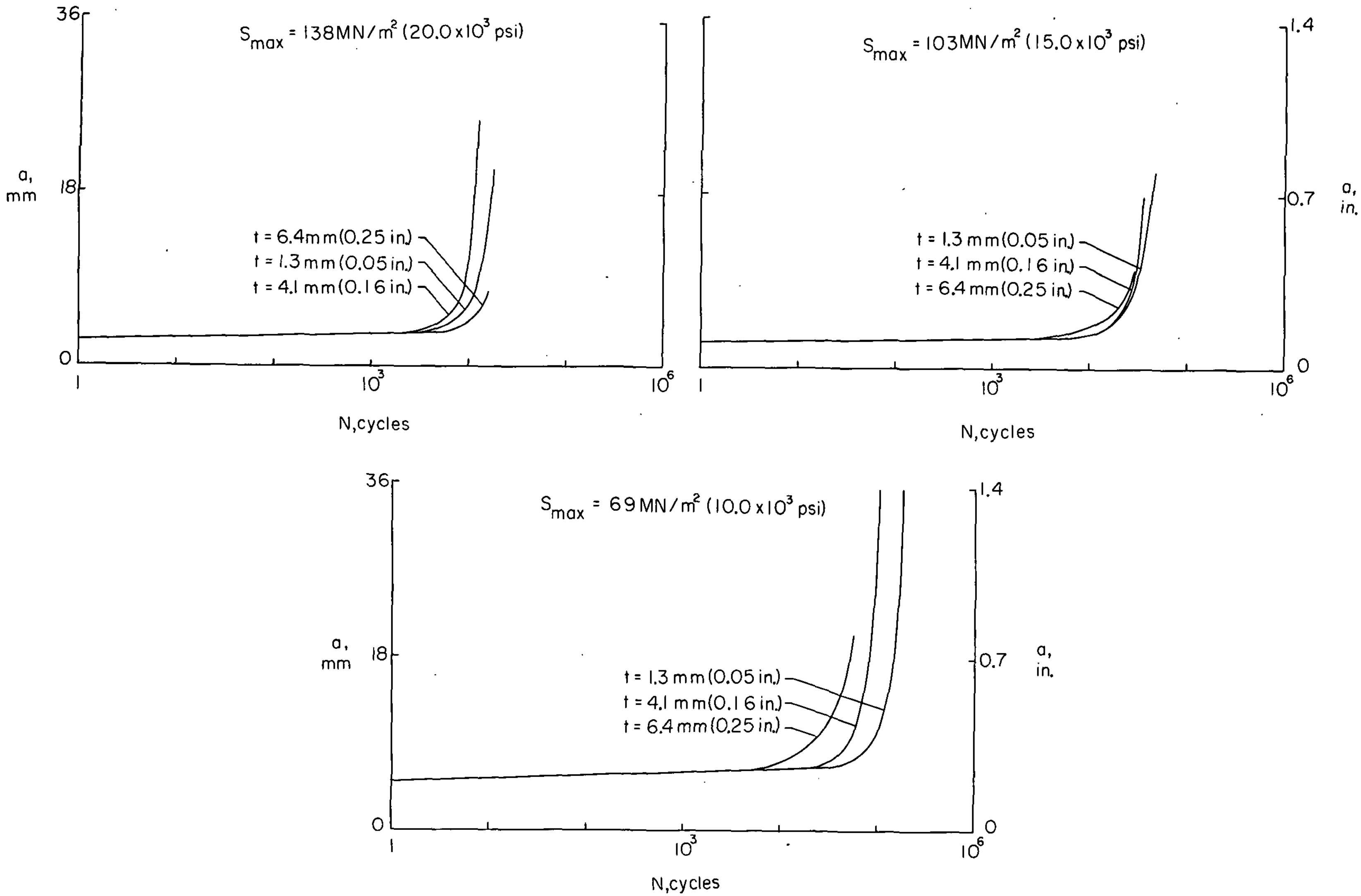

(b) R = 0.50.

Figure 3.- Concluded.

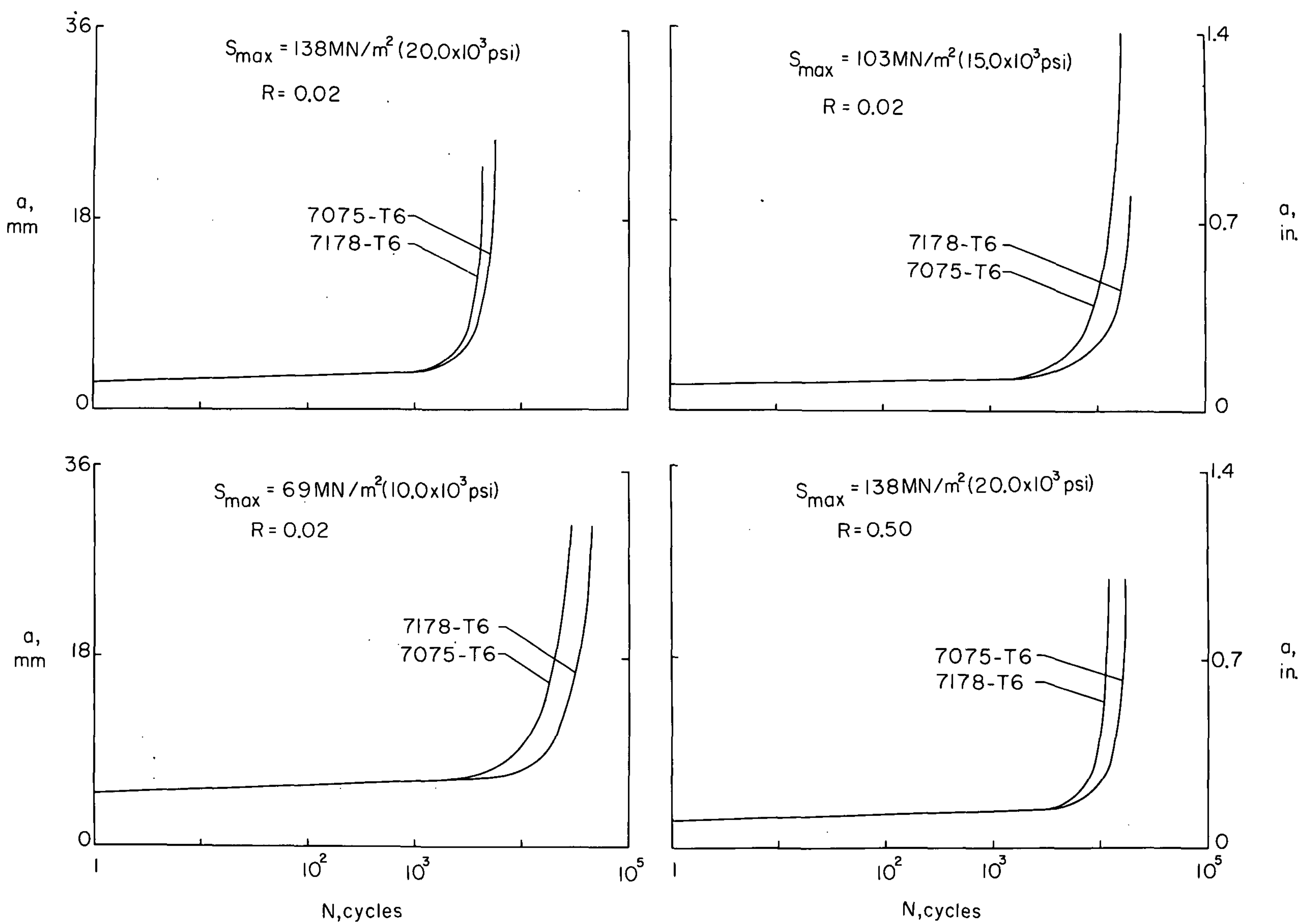

Figure 4.- Fatigue-crack-growth curves for 7075-T6 and 7178-T6 specimens of about the same thickness and tested at the same values of S_{max} and R.

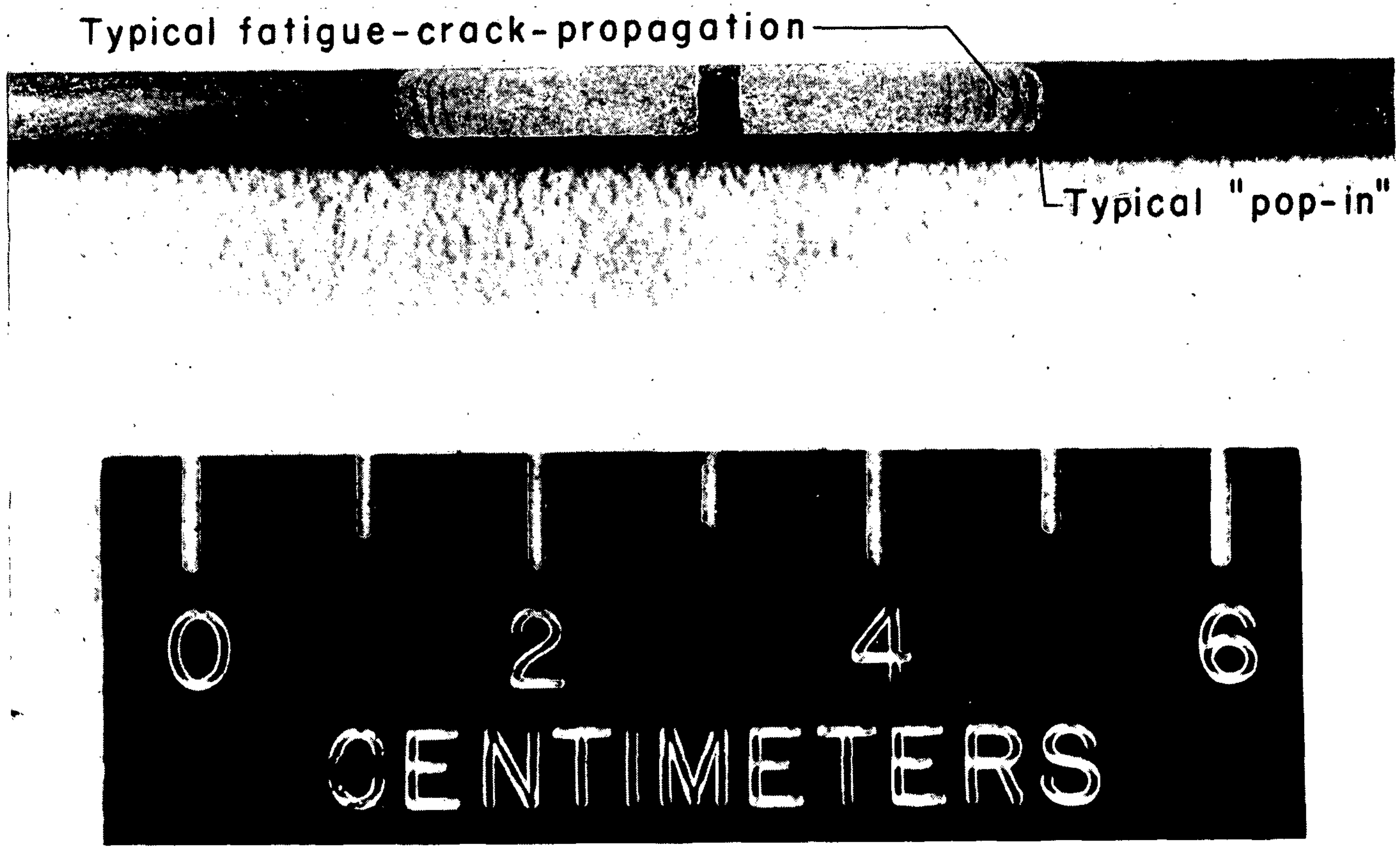

L-72-4759

(a) 7075-T6.

Figure 5.- Fracture surfaces showing pop-in.

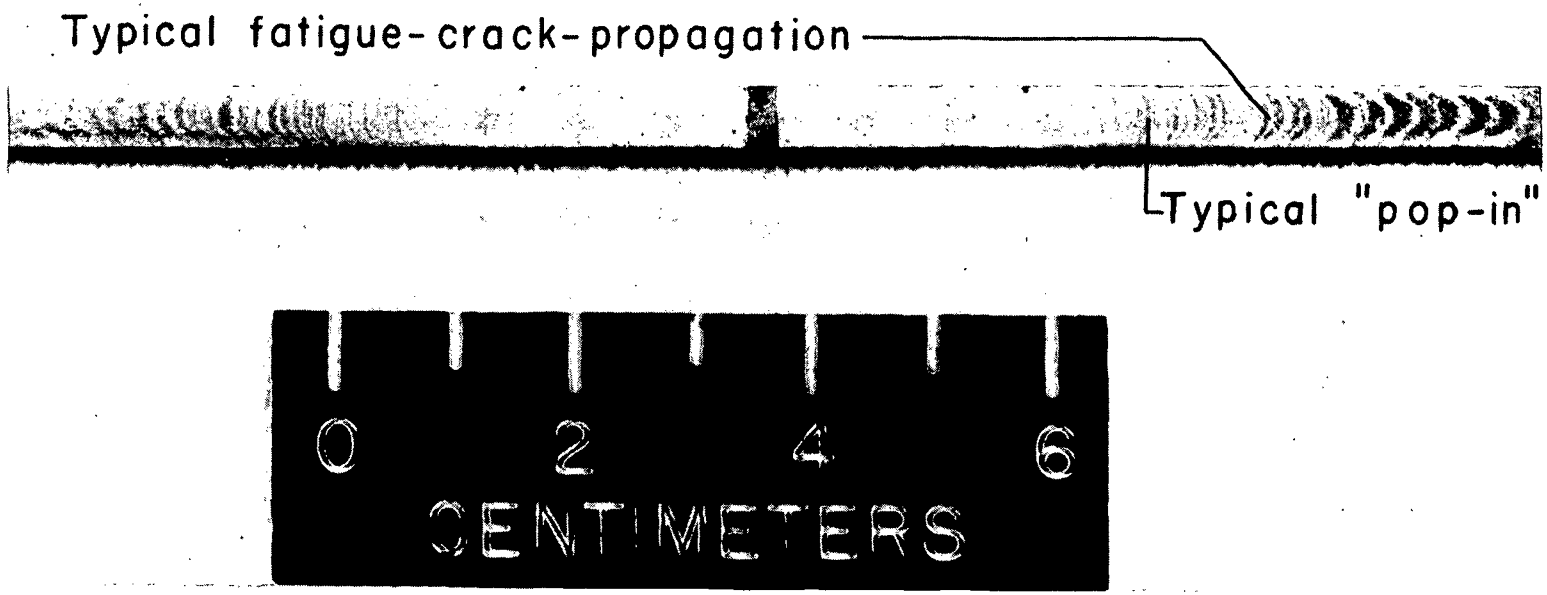

L-73-290

(b) 7178-T6.

Figure 5.- Concluded.

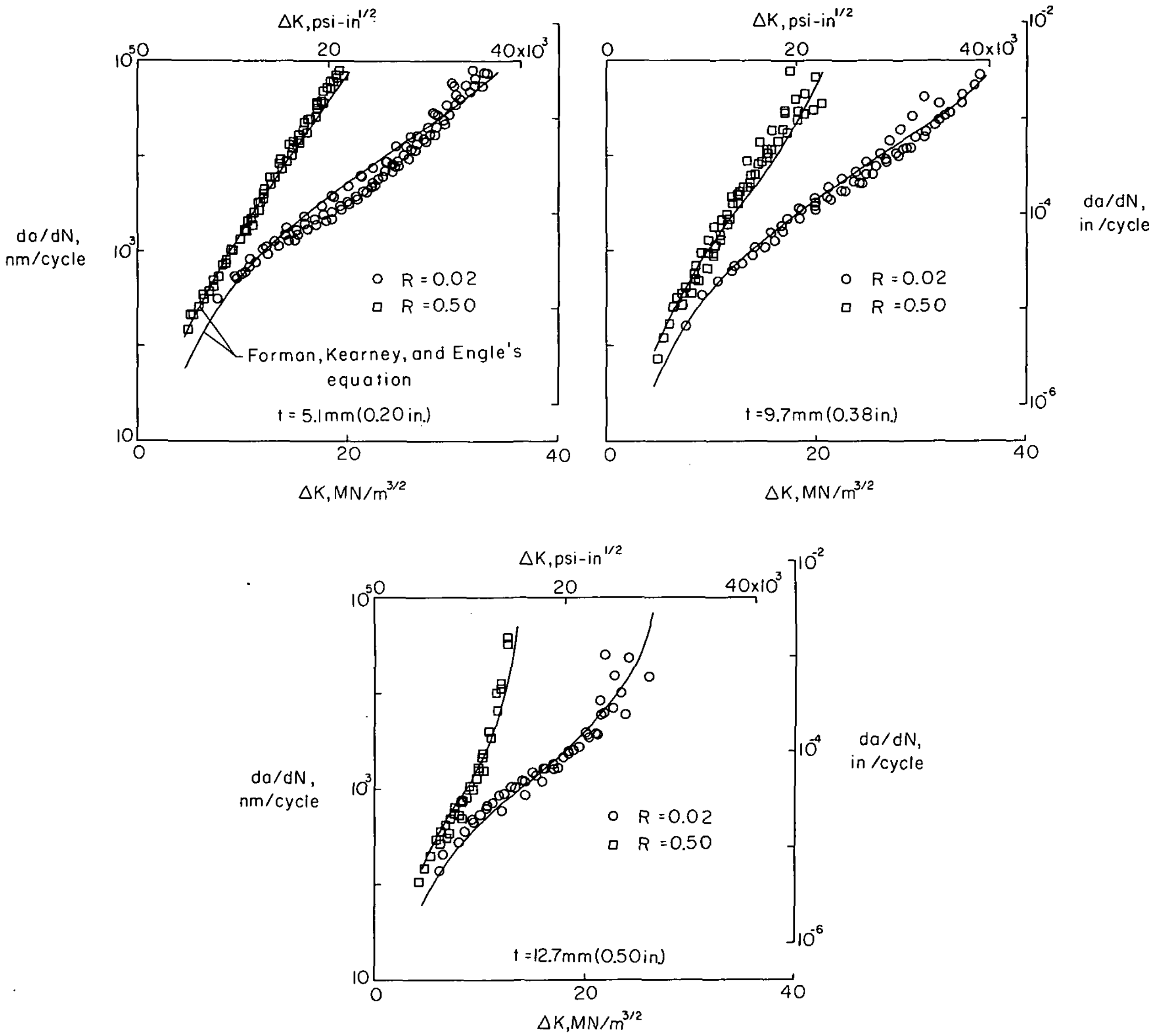

(a) 7075-T6.

Figure 6.- Variation of fatigue-crack-growth rate with ΔK for various thicknesses.

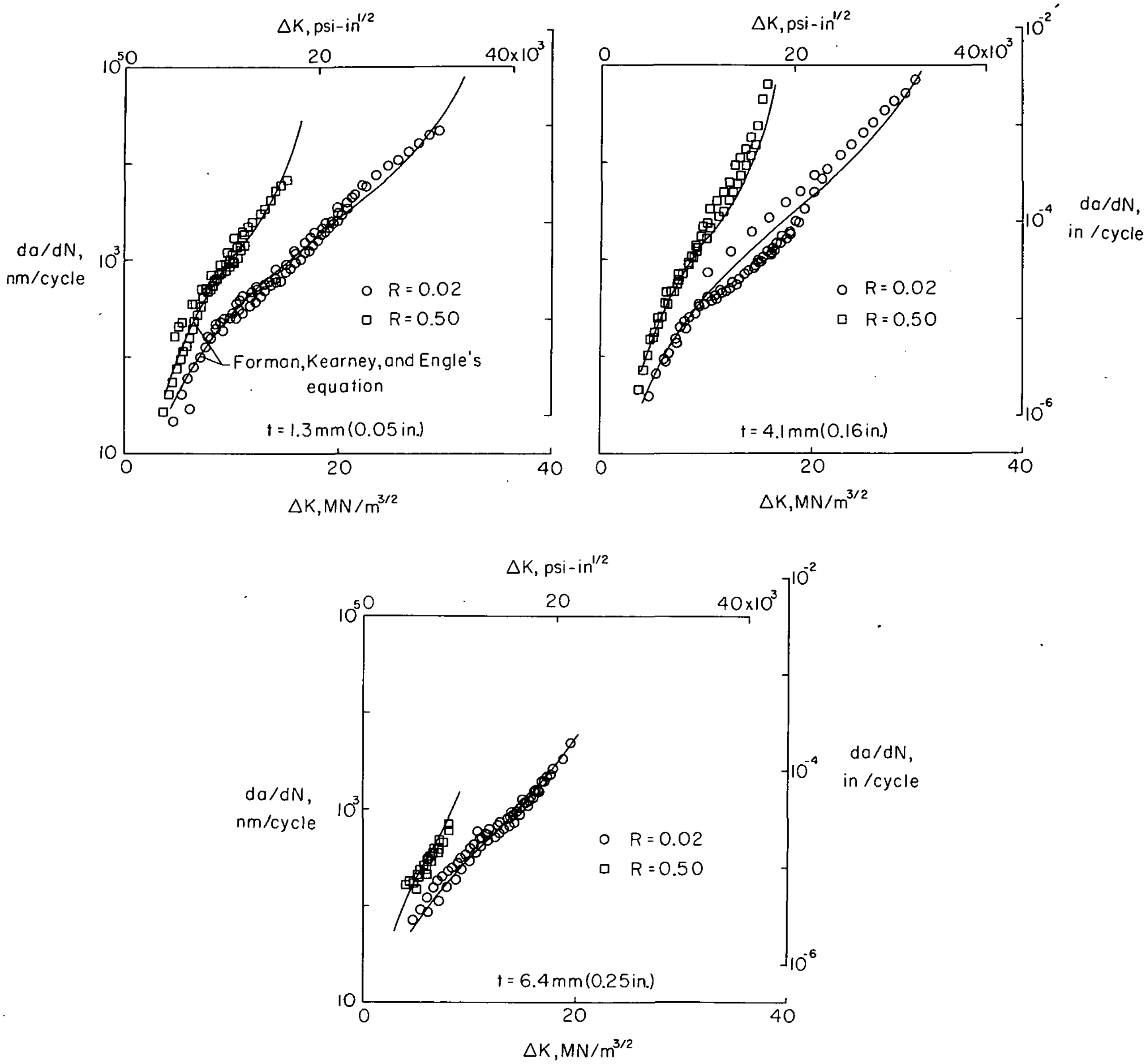

(b) 7178-T6.

Figure 6.- Concluded.

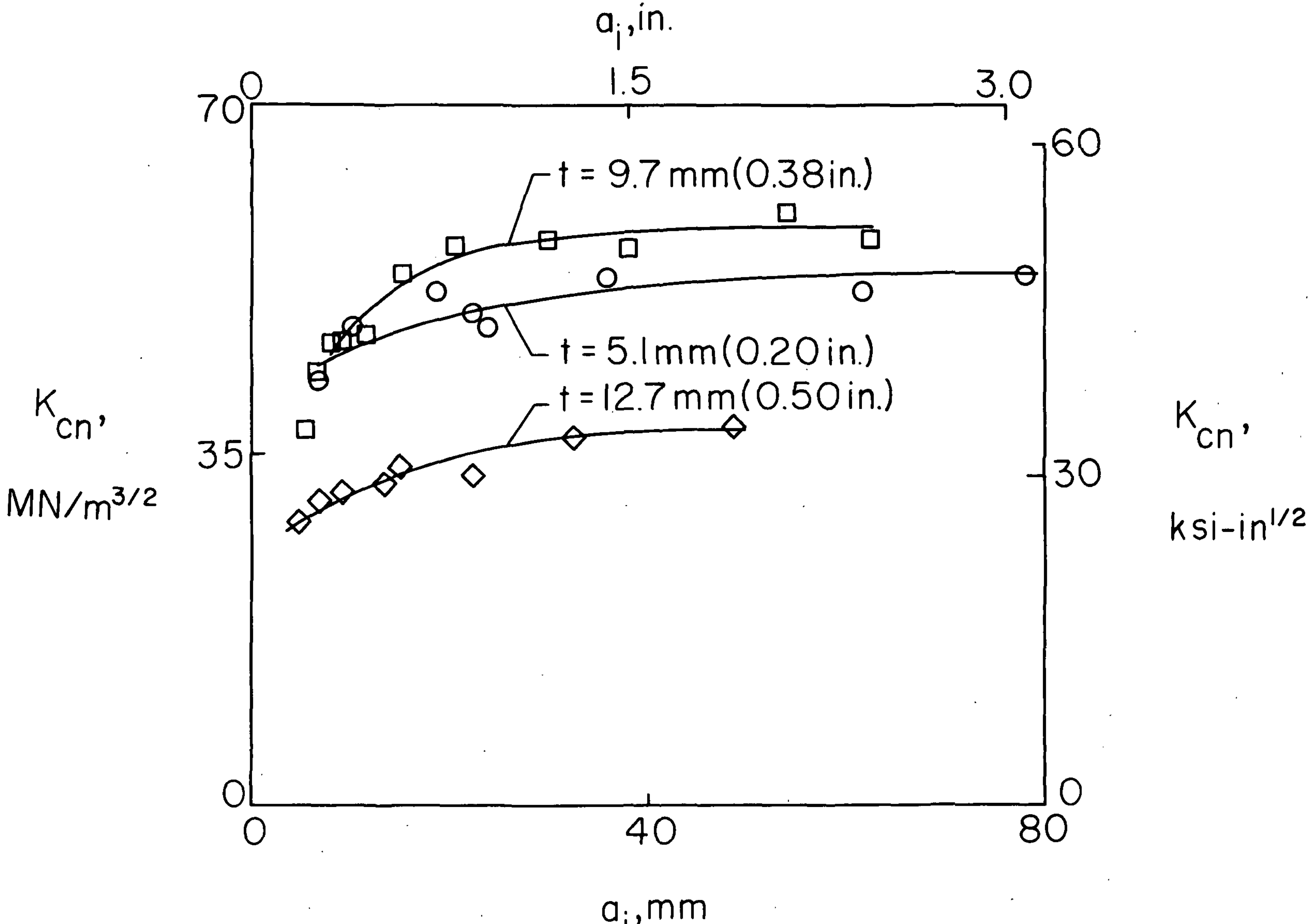

(a) 7075-T6.

Figure 7.- Variation of K_{cn} with a_i for specimens having different thicknesses.

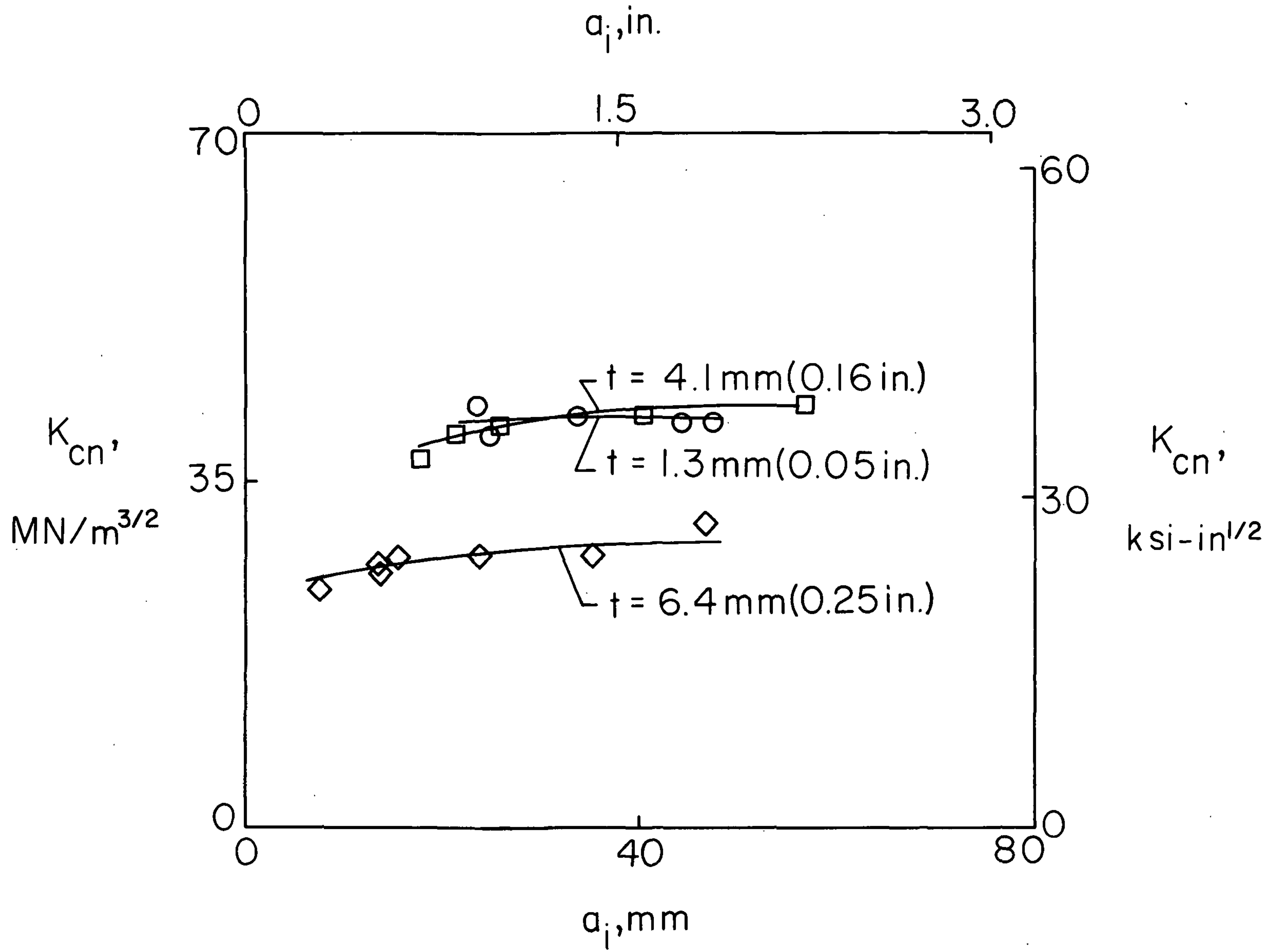

(b) 7178-T6.

Figure 7.- Concluded.

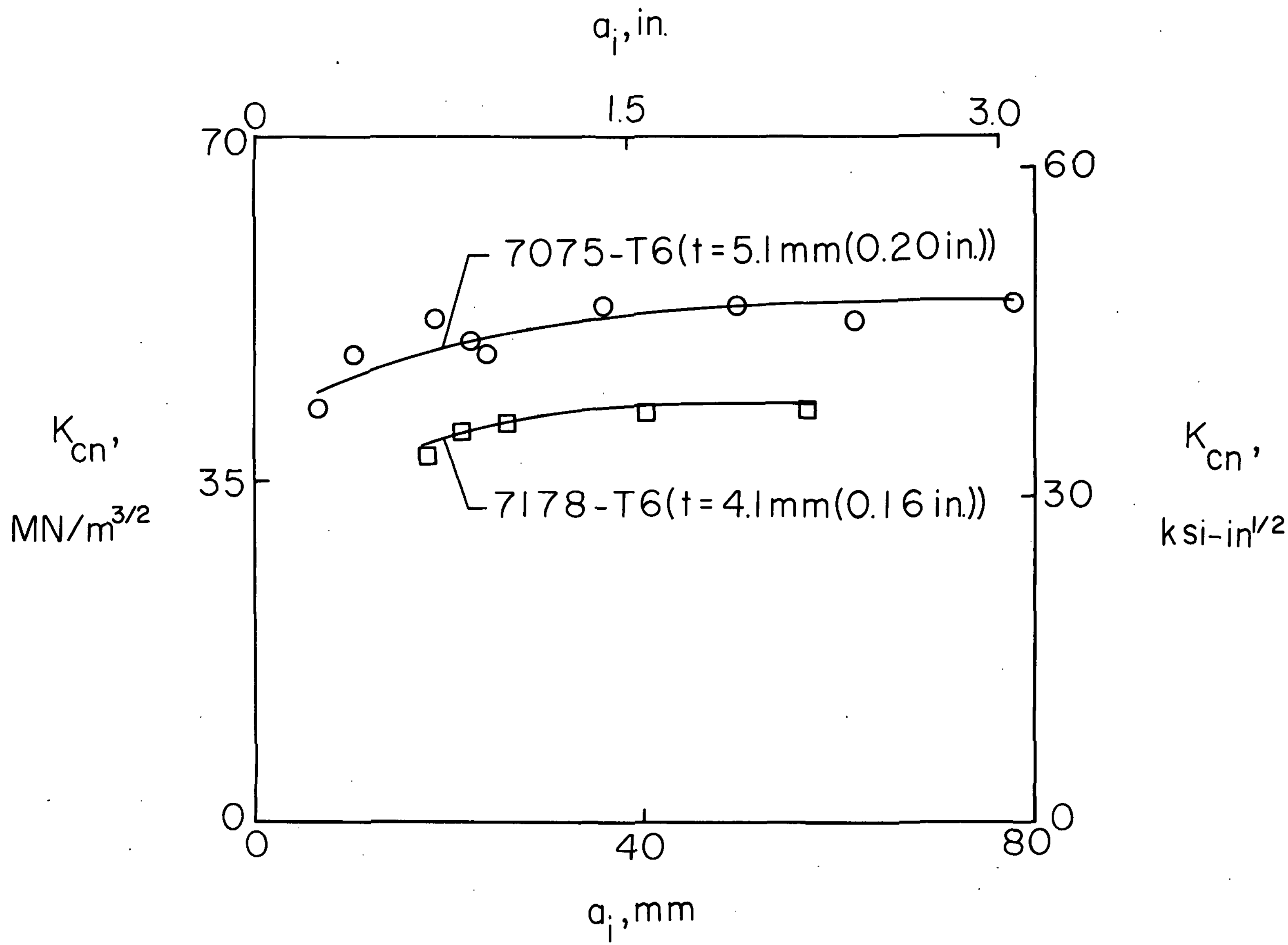

Figure 8.- Variation of K_{cn} with a_i for 7075-T6 and 7178-T6 specimens of about the same thickness.

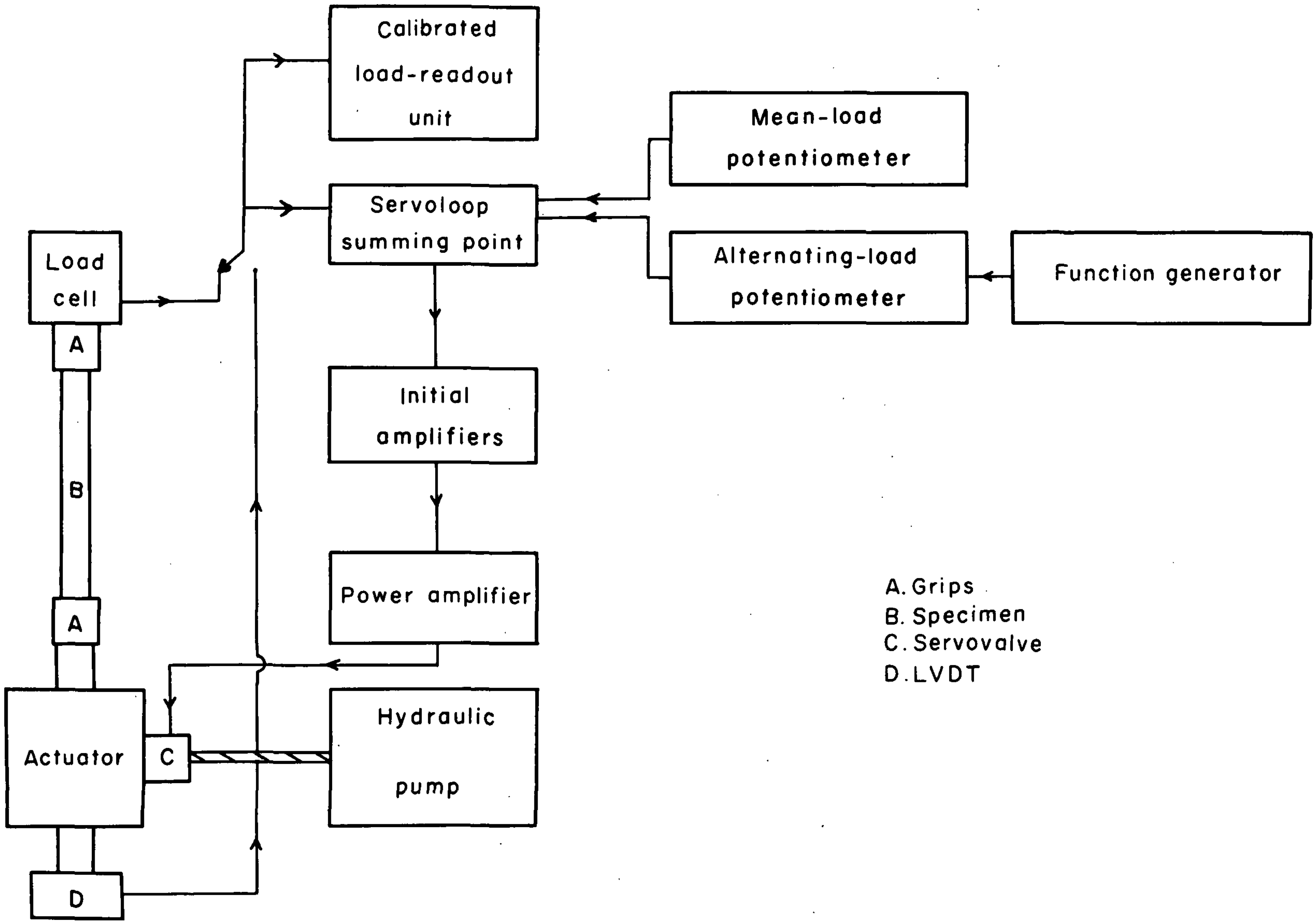

Figure 9.- Schematic diagram of loading system for 1334-kN (300 000-lbf) testing machine.

NASA-Langley, 1973 — 17 L-8731

"The aeronautical and space activities of the United States shall be conducted so as to contribute . . . to the expansion of human knowledge of phenomena in the atmosphere and space. The Administration shall provide for the widest practicable and appropriate dissemination of information concerning its activities and the results thereof."

—NATIONAL AERONAUTICS AND SPACE ACT OF 1958

NASA SCIENTIFIC AND TECHNICAL PUBLICATIONS

TECHNICAL REPORTS: Scientific and technical information considered important, complete, and a lasting contribution to existing knowledge.

TECHNICAL NOTES: Information less broad in scope but nevertheless of importance as a contribution to existing knowledge.

TECHNICAL MEMORANDUMS: Information receiving limited distribution because of preliminary data, security classification, or other reasons. Also includes conference proceedings with either limited or unlimited distribution.

CONTRACTOR REPORTS: Scientific and technical information generated under a NASA contract or grant and considered an important contribution to existing knowledge.

TECHNICAL TRANSLATIONS: Information published in a foreign language considered to merit NASA distribution in English.

SPECIAL PUBLICATIONS: Information derived from or of value to NASA activities. Publications include final reports of major projects, monographs, data compilations, handbooks, sourcebooks, and special bibliographies.

TECHNOLOGY UTILIZATION PUBLICATIONS: Information on technology used by NASA that may be of particular interest in commercial and other non-aerospace applications. Publications include Tech Briefs, Technology Utilization Reports and Technology Surveys.

Details on the availability of these publications may be obtained from:

SCIENTIFIC AND TECHNICAL INFORMATION OFFICE

NATIONAL AERONAUTICS AND SPACE ADMINISTRATION

Washington, D.C. 20546